Electronic transport and colossal electroresistance in $SrTiO_3$:Nb-based Schottky junctions

D. S. Shang, J. R. Sun,[a)] L. Shi, J. Wang, Z. H. Wang, and B. G. Shen
Beijing National Laboratory for Condensed Matter Physics and Institute of Physics, Chinese Academy of Sciences, Beijing 100190, People's Republic of China

(Received 19 December 2008; accepted 12 January 2009; published online 3 February 2009)

Current-voltage characteristics and colossal electroresistance (CER) have been experimentally investigated in the temperature range from 293 to 454 K for the Schottky junctions Au/$SrTiO_3$:0.5 wt % Nb and Au/$SrTiO_3$:0.05 wt % Nb. Both junctions show electron tunneling-dominated transport behavior. Postannealing of $SrTiO_3$:0.05 wt % Nb in oxygen atmosphere causes a transition of the transport behavior from electron tunneling to thermionic emission. The CER effect appears in the junctions with the transport behavior dominated by electron tunneling and greatly weakens when thermionic emission prevails after postannealing. This result reveals the presence of a close relation between CER and electron tunneling. © *2009 American Institute of Physics*. [DOI: 10.1063/1.3077615]

Reversible resistance switching induced by electric field, i.e., colossal electroresistance (CER) effect, in metal oxides attracted intensive attention due to its potential application to nonvolatile memories. Diverse models concerning the mechanisms of this effect have been proposed after significant experimental and theoretical efforts.[1–11] For the metal/oxide junction, a typical CER device, it is believed that the CER is due to field-induced change of Schottky-like interface.[8–12] However, it is still not clear what determines the CER characters of the materials, such as the high-to-low resistance ratio, the stability of the high/low resistance state, and the critical field required for the resistance switching.

In addition to the leakage current, there are two different currents through a Schottky junction. The first one arises from electron tunneling (ET) and the second one from thermionic emission (TE).[13] Tunneling current prevails when the depletion layer is thin or considerable defects exist in the depletion layer, while thermal current dominates transport behavior when the depletion layer is thick or the temperature is high. Considering their close relation with the junction barrier, CER and transport behavior may strongly correlate with each other. In fact, Fujii *et al.*[8] proposed a trap-assisted-tunneling origin for the CER in $SrRuO_3/SrTiO_3$:Nb (STON) junctions. However, most of the previous works focused on the CER effect alone and no special attention was paid to the electronic transport behavior of the junctions. In this letter, the transport mechanism was studied by analyzing temperature-dependent current (I)-voltage (V) characteristics of the Au/STON junctions and the relation between the CER effect and the electronic transport behavior was established.

Au/STON junctions were prepared by depositing, through a shadow mask, Au electrodes, ~400 nm in thickness and 0.2 mm in diameter, on the surface of the (001)-orientated STON crystals using magnetron sputtering following the procedure previously reported.[12] Three STON substrates were employed: two $SrTiO_3$ crystals doped with 0.5 wt % Nb (STON-1) and 0.05 wt % Nb (STON-2) and a STON-2 substrate annealed at ~600 °C for 30 min in oxygen atmosphere (STON-3). Transport data were collected using a Keithley 2601 sourcemeter. Positive bias directs from Au to STON. The temperature range investigated was from 293 to 453 K, with a temperature fluctuation smaller than 0.5 K.

Figures 1(a) and 1(b) show, in semilogarithmic scale, the I-V characteristics of Au/STON-1. The rectifying behavior and essentially linear log I-V relations for $V>0$ are typical features of the Schottky junctions. There are two remarkable anomalies worth noting. First, the log I-V curves recorded under different temperatures are parallel with each other [Fig. 1(b)]. Second, the reverse current is much larger than

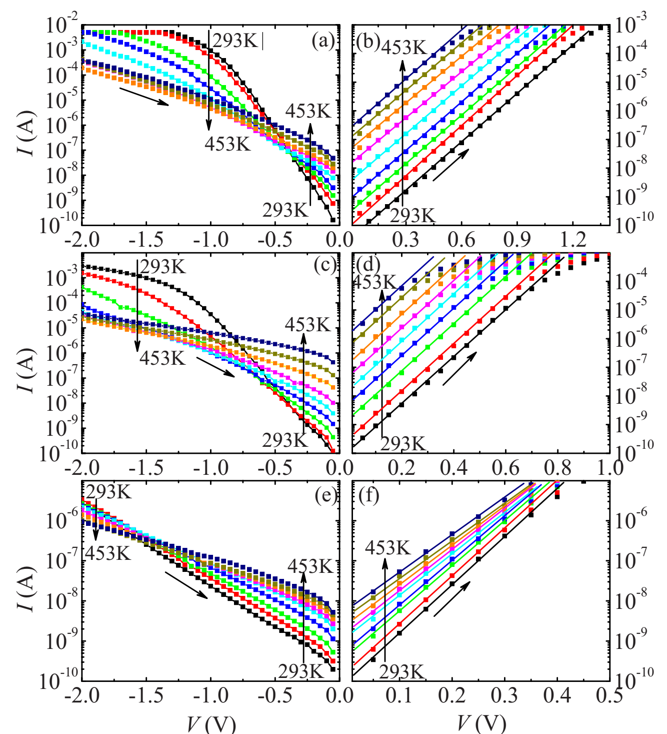

FIG. 1. (Color online) [(a) and (b)] log I-V characteristics of Au/STON-1, [(c) and (d)] Au/STON-2, and [(e) and (f)] Au/STON-3, measured in the temperature range of 293–453 K with a step of 20 K. Arrows indicate the sweeping direction of the applied field.

a)Author to whom correspondence should be addressed. Electronic mail: jrsun@g203.iphy.ac.cn.

 © 2009 American Institute of Physics

Author complimentary copy. Redistribution subject to AIP license or copyright, see http://apl.aip.org/apl/copyright.jsp

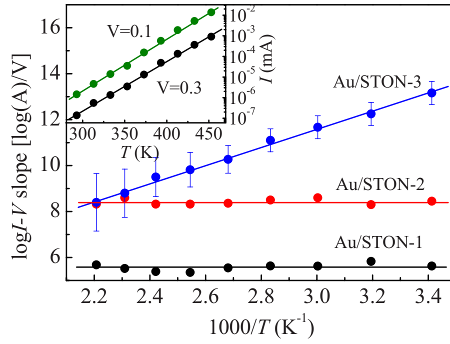

FIG. 2. (Color online) log I-V slopes as a function of temperature reciprocal. Inset: log I-T plot under two fixed bias voltages for Au/STON-1.

the expected saturation current and undergoes a crossover from increase to decrease with temperature as reverse bias grows. These results reveal the deviation of the transport behavior of Au/STON-1 from the standard TE process. Similar features, except for minor differences in detailed I-V dependence, are observed in Au/STON-2 [Figs. 1(c) and 1(d)]. Compared to the first two junctions, Au/STON-3 exhibits obviously different I-V characteristics [Figs. 1(e) and 1(f)]. Although linearity remains in the log I-V curves for $V>0$, the log I-V slope displays a strong dependence on temperature, decreasing with increasing temperature. Reverse current is also much lower than that of Au/STON-1 and Au/STON-2.

The electronic transport behavior of Au/STON-1 and Au/STON-2 can be well described by the Newman equation, $I \propto \exp(\alpha T)\exp(\beta V)$, where α and β are constants weakly dependent on temperature and voltage.[14] This equation predicts a log I-V slope independent of temperature and a linear increase in log I with temperature when bias voltage is fixed, as observed in manganite/STON junctions.[15] log I-V slope as a function of temperature reciprocal is shown in Fig. 2. It is ~5.8 log (A)/V and ~8.2 log (A)/V for Au/STON-1 and Au/STON-2, respectively, essentially independent of temperature. The exponential growth of current with temperature is also observed under fixed voltages (inset in Fig. 2). These features are consistent with those predicted by the Newman equation and strongly suggest the ET characters of the transport behavior in both junctions. The lower log I-V slope in Au/STON-1, compared with Au/STON-2, may indicate a higher build-in field in the former junction, which is consistent with the fact that the doping level of STON-1 is larger than that of STON-2. In contrast with the former two junctions, the log I-V slope of Au/STON-3 varies with temperature in the form of q/nk_BT with $n \approx 1.3$, where q is the electron charge, n is the ideality factor, and k_B is the Boltzmann constant. This result reveals the TE-character of the transport behavior, for which the forward current is given by $I_F \propto \exp(qV/nk_BT)$.[13]

To get an insight into the relation between CER and the TE/ET behavior, the field-induced resistance changes are further studied. Figures 3(a)–3(c) show the I-V curves measured at different temperatures for the voltage cycling of $0 \rightarrow +2\ \text{V} \rightarrow 0 \rightarrow -2\ \text{V} \rightarrow 0$ (sweeping speed=50 mV/s). For clarity, only two representative I-V curves, corresponding to T=293 and 453 K, respectively, are presented for each junction. The obvious I-V hysteresis observed in Au/STON-1 and Au/STON-2 indicates nonvolatile resistance changes. In contrast, no obvious I-V hysteresis occurs for Au/STON-3.

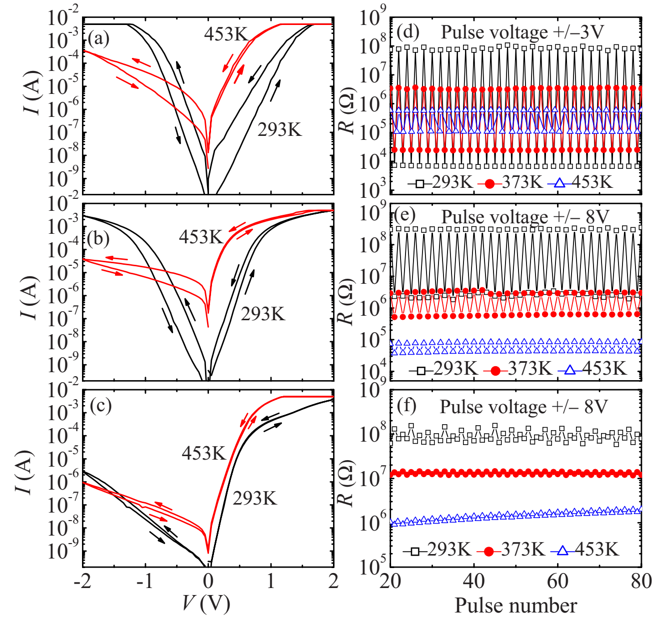

FIG. 3. (Color online) Electroresistance induced by voltage cycling (left panel) and voltage pulses (right panel). Only the I-V curves collected under 293 and 453 K are presented for clarity. (a) and (b): Au/STON-1. (c) and (d): Au/STON-2. (e) and (f): Au/STON-3.

Resistance change can also be induced by electric pulses. Positive and negative voltage pulses, 1 ms in width, were alternatively applied to the junctions and the resistance was recorded under the bias of 0.1 V immediately after each pulse. The pulse amplitudes of 3 V (for Au/STON-1) and 8 V (for Au/STON-2 and Au/STON-3) were selected, which are the highest voltages without causing permanent breakdown. As expected, the junction resistances of Au/STON-1 and Au/STON-2 are greatly modified by electric pulses, while that of Au/STON-3 is insensitive to the pulses [Figs. 3(d)–3(f)]. Figure 4 shows the CER ratio, defined as $\text{ER}=(R_{high}-R_{low})/R_{low}$, as a function of temperature. The inset plot in Fig. 4(a) illustrates the calculation of the ER ratio based on the I-V curves. The strongest CER effect takes place in Au/STON-1 and the maximum ER values, near the ambient temperature, are ~10 000% and ~1 000 000%, produced by voltage cycling and voltage pulse, respectively. The CER effect of Au/STON-2 is comparable with that of Au/STON-1,

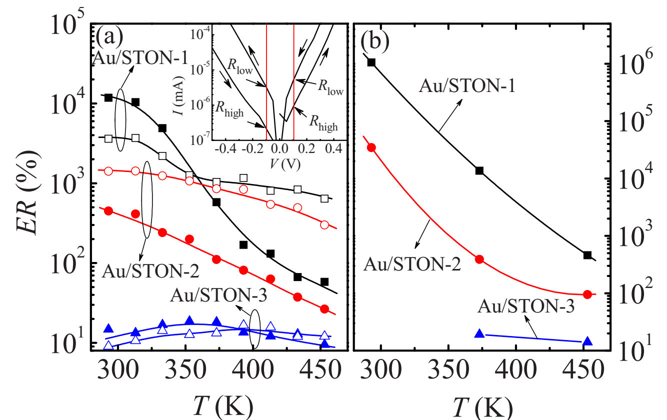

FIG. 4. (Color online) ER values induced by (a) voltage cycling and (b) voltage pulses. Inset: Schematic for the determination of $\text{ER}=(R_{high}-R_{low})/R_{low}$ induced by voltage cycling mode. Solid and open symbols in (a) represent, respectively, the ER values measured at 0.1 and −0.1 V.

Author complimentary copy. Redistribution subject to AIP license or copyright, see http://apl.aip.org/apl/copyright.jsp

though the ER values are slightly smaller. Different from the former two junctions, the electroresistance of Au/STON-3 is the lowest, and the ER values are generally below 20%. These results indicate that the CER effect appears only in the junctions with the transport behavior dominated by ET and greatly weakens when TE prevails, despite the decrease in the ER values with increasing temperature.

Occurrence of ET indicates that the depletion layers of Au/STON-1 and Au/STON-2 are quite thin and, furthermore, considerable defects that assist ET may exist in this layer. We measured the junction capacitance at a frequency of 1 kHz at ambient temperature and obtained the values of ~4.2, ~3.2, and ~2 nF for Au/STON-1, Au/STON-2, and Au/STON-3, respectively. The relative permittivity should be different for the three samples due to different built-in electric fields. According to the data given by van der Berg *et al.*,[16] it is approximately ~50, ~100, and ~300, respectively, for STON-1, STON-2, and STON-3. The effective thickness of the depletion layer W can be calculated following the formula $C=\varepsilon_0 \varepsilon S/W$, and it is ~33, ~87, and ~415 Å, respectively, for the three junctions, where ε is the relative permittivity of the depletion layer and $S \approx 0.0314$ mm^2 is the area of the junction. The different transport behaviors in the three samples can therefore be understood. Electrons prefer to tunnel through interfacial barrier for Au/STON-1 and Au/STON-2, because of the thin depletion layer, and to surmount interfacial barrier for Au/STON-3, due to the thick depletion layer. According to the semiconductor theory, external electric field is completely applied to the depletion layer. A smaller depletion width means a higher electric field in the depletion layer, as the case occurred in Au/STON-1 and Au/STON-2. High electric fields, together with the defects in the depletion layer, would promote the formation of conducting filaments. It has been reported that the anionic/cationic vacancies (ions), which act as dopants, exhibit very high mobility near crystalline defects, and their rearrangements under external field are feasible.[17] Based on the photoresponse experiments, we demonstrated the dominant role of conducting paths on the CER effect.[12] With these in mind, we can conclude that both the CER effect and the ET-like transport behavior are the natural consequences of thin depletion layers of the junctions.

Based on the above analysis, the different CER effects in Au/STON-1, Au/STON-2, and Au/STON-3 can be understood. The CER effect in Au/STON-1 is the strongest among the three samples because Au/STON-1 has the thinnest depletion layer, thus the highest electric field. The CER of Au/STON-2 is obviously smaller than that of Au/STON-1. The depletion layer of Au/STON-2 is ~2.6 times larger than that of Au/STON-1. Postannealing in oxygen atmosphere eliminates the donorlike defects, for example, oxygen vacancies, in the vicinity of the Au/STON-3 interface, which causes a growth in the depletion layer. As a consequence, the CER effect is greatly suppressed.

It should be noted that the spatial fluctuation of defect distribution is also reduced by increasing depletion width. In this case, it is difficult to induce local rearrangements of anionic/cationic vacancies (ions), thus resistance switching simply by increasing the amplitude of the electric pulses. This may explain the absence of the CER effect in high electric field for Au/STON-3. As a supplement, we would like to point out that the CER effect becomes weak at elevated temperatures. This may be caused by the decrease in the initial junction resistance at high temperatures.

In summary, temperature dependent *I-V* characteristics were experimentally investigated for three types of $Au/SrTiO_3$:Nb Schottky junctions. It was demonstrated that the electronic transport is dominated by ET and TE for the junctions with thin and thick depletion layers, respectively. The CER occurs only in the junctions that show the ET-dominant behavior. The present work reveals possible approaches toward enhancing the CER effect in the junctions.

The authors would like to thank S. L. Li for his assistance in sample preparation. This work has been supported by the National Basic Research of China, the National Natural Science Foundation of China, the Knowledge Innovation Project of the Chinese Academy of Sciences, the Beijing Municipal Natural Science Foundation, and the China Postdoctoral Science Foundation.

[1] A. Beck, J. G. Bednorz, Ch. Gerber, C. Rossel, and D. Widmer, Appl. Phys. Lett. **77**, 139 (2000).
[2] A. Odagawa, H. Sato, I. H. Inoue, H. Akoh, M. Kawasaki, Y. Tokura, T. Kanno, and H. Adachi, Phys. Rev. B **70**, 224403 (2004).
[3] M. J. Rozenberg, I. H. Inoue, and M. J. Sánchez, Phys. Rev. Lett. **92**, 178302 (2004); Appl. Phys. Lett. **88**, 033510 (2006).
[4] D. S. Shang, Q. Wang, L. D. Chen, R. Dong, X. M. Li, and W. Q. Zhang, Phys. Rev. B **73**, 245427 (2006).
[5] I. H. Inoue, S. Yasuda, H. Akinaga, and H. Takagi, Phys. Rev. B **77**, 035105 (2008).
[6] S. C. Chae, J. S. Lee, S. Kim, S. B. Lee, S. H. Chang, C. Liu, B. Kahng, H. Shin, D. W. Kim, C. U. Jung, S. Seo, M. J. Lee, and T. W. Noh, Adv. Mater. (Weinheim, Ger.) **20**, 1154 (2008).
[7] M. C. Ni, S. M. Guo, H. F. Tian, Y. G. Zhao, and J. Q. Li, Appl. Phys. Lett. **91**, 183502 (2007).
[8] T. Fujii, M. Kawasaki, A. Sawa, Y. Kawazoe, H. Akoh, and Y. Tokura, Phys. Rev. B **75**, 165101 (2007).
[9] A. Sawa, Mater. Today **11**, 28 (2008).
[10] C. Park, Y. Seo, J. Jung, and D. W. Kim, J. Appl. Phys. **103**, 054106 (2008).
[11] A. Ruotolo, C. W. Leung, C. Y. Lam, W. F. Cheng, K. H. Wong, and G. P. Pepe, Phys. Rev. B **77**, 233103 (2008).
[12] D. S. Shang, J. R. Sun, L. Shi, and B. G. Shen, Appl. Phys. Lett. **93**, 102106 (2008); D. S. Shang, J. R. Sun, L. Shi, Z. H. Wang, B. G. Shen, *ibid.* **93**, 172119 (2008).
[13] S. M. Sze and K. K. Ng, *Physics of Semiconductor Devices*, 3rd ed. (Wiley, New Jersey, 2007).
[14] B. L. Sharma and R. K. Purohit, *Semiconductor Heterojunctions* (Pergamon, Oxford, 1974), pp. 1–13.
[15] Y. W. Xie, J. R. Sun, D. J. Wang, S. Liang, W. M. Lü, and B. G. Shen, Appl. Phys. Lett. **90**, 192903 (2007).
[16] R. A. van der Berg, P. W. M. Blom, J. F. M. Cillessen, and R. M. Wolf, Appl. Phys. Lett. **66**, 697 (1995).
[17] K. Szot, W. Speier, G. Bihlmayer, and R. Waser, Nature Mat. **5**, 312 (2006); R. Waser and M. Aono, *ibid.* **6**, 833 (2007); J. J. Yang, M. D. Pickett, X. Li, D. A. A. Ohlberg, D. R. Stewart, and R. S. Williams, Nat. Nanotechnol. **3**, 429 (2008).

Author complimentary copy. Redistribution subject to AIP license or copyright, see http://apl.aip.org/apl/copyright.jsp